Princeton Plasma Physics Laboratory

NSTX Experimental Proposal

Title: NSTX - DIII-D RWM Similarity Experiment

OP-XP-512	**Revision: v1.10**	Effective Date: 5/15/05 *(Ref. OP-AD-97)* Expiration Date: *(2 yrs. unless otherwise stipulated)*

PROPOSAL APPROVALS

Author: Aaron Sontag	Date
ATI – ET Group Leader: D. Gates	Date
RLM - Run Coordinator: J. Menard	Date **May 16, 2005**

Responsible Division: Experimental Research Operations

Chit Review Board (designated by Run Coordinator)

MINOR MODIFICATIONS (Approved by Experimental Research Operations)

NSTX EXPERIMENTAL PROPOSAL

NSTX - DIII-D RWM Similarity Experiment **OP-XP-512**

Authors: A. Sontag, S. Sabbagh, H. Reimerdes, A. Garofalo, W. Zhu, J. Menard, K. Shaing, E. Strait, R. La Haye, Y. Liu

1. Overview of planned experiment

The purpose of this experiment is to examine the effects of aspect ratio on the rotational stabilization and mode dynamics of the resistive wall mode (RWM) by comparing the RWM characteristics measured during similar NSTX and DIII-D discharges. Understanding the aspect ratio dependence of these differences in RWM behavior will help to confirm or deny the leading theories currently used to explain RWM stability and the dynamic behavior of the plasma in the presence of an RWM. The present experiment will look at differences in RWM physics due to a change from low to moderate aspect ratio by producing NSTX discharges with a poloidal cross-section and proximity to the no-wall beta limit similar to that of DIII-D.

This experiment will study differences due to plasma aspect ratio in:

1) Critical plasma rotation frequency for MHD stability
2) Passive RWM stability limits (maximum C_β w/o active feedback)
3) RWM growth rate and mode rotation frequency
4) Magnetic braking and rotation damping profile
5) Resonant field amplification

The comparable experiment was proposed and run on DIII-D as D3DMP No 2005-04-58 on 2/14/05 and 3/17/05. The NSTX shape was matched well in an appropriate configuration for RWM studies in NSTX. Valuable information on the above areas of comparison was obtained, providing guidance for this proposal.

2. Theoretical/ empirical justification

There are several experimentally observed and theoretically predicted RWM characteristics which vary with aspect ratio and can be used to validate RWM theories:

Mode structure & dynamics:

The structure of the RWM is altered by the magnetic geometry of low aspect ratio. The high pitch of the magnetic field lines on the inboard side of the plasma leads to a theoretically predicted increase in the local poloidal wavelength of the RWM in NSTX as compared to DIII-D[1]. Also the n=1 RWM has been observed to couple to higher toroidal harmonics in

NSTX. This experiment will compare the mode structure variation with aspect ratio while other geometric variables are held constant. The addition of MSE current profile constraint during EFIT reconstructions will lead to a more accurate theoretical calculation of the mode structure in NSTX than has been possible previously. Also the USXR detector arrays and internal profile diagnostics (Thomson, CHERS) will provide confirmation of the calculated mode structure by verifying the extent of the perturbation and its effects on the plasma temperature and rotation.

The RWM causes strong, global plasma rotation damping, which is a key element of the dynamic process through which the RWM causes a beta collapse. So understanding the effects of the mode structure on the rotation damping is important to sustained high beta operations. The magnitude of this damping can be estimated using a neoclassical toroidal viscosity (NTV) model in both NSTX[2] and DIII-D[3]. The NTV torque on the plasma due to a dominant mode with poloidal and toroidal mode numbers of m and n respectively is given by:

$$T_{NTV} = R\frac{\pi^{1/2} p_i}{\nu_{ti}}\left(\Omega_\phi - \Omega_{\mathrm{mod}\,e}\right)\varepsilon^2 n^2 q\left(\frac{\delta B_r^{mn}}{B_\phi}\right)^2$$

The estimated torques agree well with the measured values given assumptions about the magnitude and structure of the magnetic perturbations inside the plasma. XP524 "Active Control of Rotation Damping in NSTX plasmas" by W. Zhu, et al. will examine the dependence of RWM-induced plasma rotation damping on mode parameters. However, it is left to the present experiment to examine the aspect ratio dependence of this damping. Examining the rotation damping dynamics between similar discharges in NSTX and DIII-D should help reveal the aspect ratio dependence of the NTV model and allow comparison of theory to experiment.

Critical rotation:

The minimum toroidal plasma rotation frequency required to stabilize the RWM is defined as the critical rotation frequency (Ω_{crit}). There are two theories which currently give a scaling that agrees with the values of Ω_{crit} observed in NSTX and DIII-D.

A drift-kinetic stability model of the RWM developed by Bondeson and Chu[4] found that a plasma with a toroidal rotation speed which satisfies the inequality $\omega_{rot} > \omega_A/4q^2$ will experience a modification of the Alfven eigenmode structure because of enhanced toroidal inertia. This modification of the eigenmode structure allows increased dissipation of the energy driving the RWM unstable and is thus stabilizing. However, the above expression was derived using a high-A approximation. If one includes neoclassical effects, it can be shown that Ω_{crit}/ω_A has an inverse dependence on aspect ratio[5].

Considering Fitzpatrick-Aydemir (F-A) RWM stability theory[6], Ω_{crit}/ω_A has a 1/q dependence. The addition of neoclassical viscosity to the F-A model includes the toroidal inertial enhancement effect and gives a critical rotation of $\Omega_{crit} \sim \varepsilon^\alpha/q^2$ where α may vary from 1 to 0.25 depending on the RWM dissipation strength.

Ω_{crit} has been measured in DIII-D and NSTX using different techniques. Without error field correction, DIII-D discharges typically experience magnetic braking when $\beta_N > \beta_N^{no\text{-}wall}$ due to resonant field amplification. As the rotation drops, DIII-D measures Ω_{crit} by noting the plasma rotation at which the RWM starts to grow. A $1/q^2$ dependence for Ω_{crit} is consistent with DIII-D measurements so far as shown in Figure 1. Analysis of CY2004 NSTX data indicated that the RWM was rotationally stabilized most of the time when $\beta_N > \beta_N^{no\text{-}wall}$ with no signs of steady rotation braking due to error fields[7]. So the stability boundary was determined for NSTX by examining the lower boundary of a scatter plot showing the rotation for a set of discharges which were rotationally stabilized for periods >> τ_{wall}. This method gives a similar n/q^2 scaling, but the coefficient is different (n = 0.25 for NSTX and n = 0.1 for DIII-D[8]) and may be due to aspect ratio effects.

Application of an external n = 1 perturbation on NSTX will allow for controlled rotation braking leading to induced RWM instability by reaching Ω_{crit} at desirable times, i.e. during tearing mode MHD quiescent periods. Controlled rotation braking will also allow the critical rotation boundary to be mapped out using a similar method as DIII-D, allowing a direct comparison between machines.

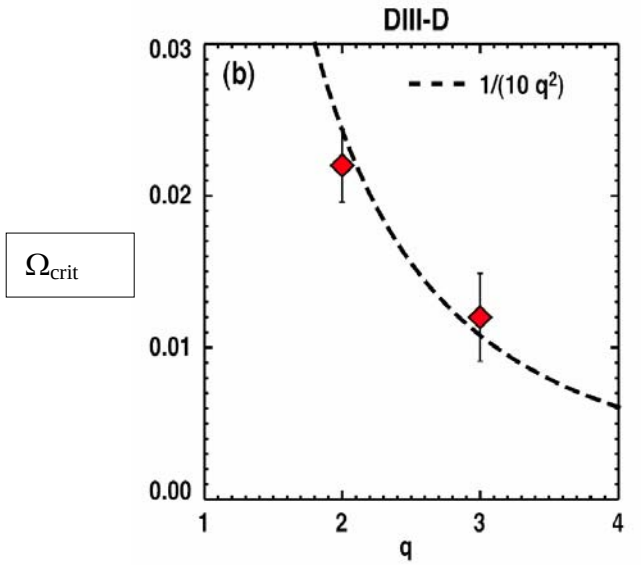

Figure 1: DIII-D critical rotation variation with q

Active study of RWM characteristics:

Experiments on DIII-D have determined the plasma response to the application of both AC and DC radial n = 1 external fields as a function of normalized beta and other parameters. The excitation of a stable plasma response by this method is referred to as resonant field

amplification (RFA[9]). The RFA has been modeled by an empirical single mode model[10], as well as a simple theoretical model[11]. The RFA amplitude predicted by these models is dependent on the plasma rotation frequency as well as characteristics of the plasma such as the level of dissipation, the plasma stability to the RWM (i.e. proximity of the plasma to the no-wall beta limit), and the mode growth rate and rotation frequency. By scanning the rotation frequency of the applied error field and varying β_N, the measured RFA can be used to determine the mode growth rate and rotation frequency as well as estimate the level of dissipation from these models using the Fitzpatrick model formalism[12]. Also the ability of these models to accurately describe the observed behavior of the RFA provides a test of the adequacy of each model. The toroidal coupling of n > 1 modes in NSTX could require the use of a multi mode model rather than the single mode model to adequately describe the data. The ability of the theoretical model to describe the RFA data will provide an indication of the completeness of this theory.

Initial RFA experiments on NSTX using the 2 error field coils available during the CY2004 run produced encouraging results showing an RFA increase with increasing β_N as expected. The measured RFA values for NSTX were similar in magnitude to those observed by DIII-D. XP501 "MHD Spectroscopy of Wall-stabilized High Beta Plasmas" by S.A. Sabbagh, et al. will perform a detailed analysis of RFA in NSTX due to both DC and AC fields for the first time using the full RWM coil set. The present experiment will focus on using the techniques explored in XP501 in an NSTX discharge which has a similar cross-section and wall proximity to DIII-D to allow a direct comparison of these results between the two machines to examine the aspect ratio effects on RWM growth rate, natural rotation frequency, and magnitude of dissipation.

RWM stability dependence on v_A and C_s:

An aspect ratio scan will allow variation of the parameters which affect the strength of the stabilizing energy dissipation. There are two leading models for energy dissipation mechanisms, a sound wave damping model[13] and a kinetic damping model[4]. In the sound wave damping model, the plasma energy driving the RWM unstable couples to sound waves through the perturbed plasma toroidal velocity. The sound waves are subsequently dissipated via ion Landau damping. The coupling between the plasma rotation and the sound waves is maximized when $v_\phi \sim C_s$ and the subsequent ion Landau damping is increased with increasing $k_\| v_{ti}$. The kinetic damping model is that of Bondeson and Chu[4] discussed in the critical rotation section of this proposal. This model describes energy dissipation through Landau damping with a similar v_{ti} dependence. To test which of these mechanisms is dominant in stabilizing the RWM, it is desirable to scan the sound speed, $C_s \propto [T_e/m_i]^{1/2}$, and the Alfven speed, $v_A = B/[4\pi n_i m_i]^{1/2}$, independently. With a large difference in field between the two machines, there is already a large variation in the Alfven speed between NSTX and DIII-D. More data points can be added to this comparison by scanning the toroidal field at constant q which, assuming the falloff in T_e is slower than the drop in B, will make it possible to vary the sound speed and the Alfven speed independently in NSTX.

References:

1) S.A. Sabbagh, et al., Phys. Plasmas **9** 2085 (2002)

2) W. Zhu, Bull. Am. Phys. Soc. **49**, 68 (2004)

3) R.J. La Haye, Nucl. Fusion, **44** 1197 (2004)

4) A. Bondeson, M.S. Chu, Phys. Plasmas **3**, 3013 (1996)

5) K. Shaing, pvt. comm.; Sabbagh IEA Workshop 59, General Atomics, Feb. 2005

6) R. Fitzpatrick, Nucl. Fusion **7** 1049 (1993)

7) S.A. Sabbagh, et al., Conference Proceedings, 20th IAEA Fusion Eneergy Conference, Vilamoura, Portugal, (IAEA, Vienna, 2004)

8) A.C. Sontag, et al., Phys. Plasmas **12**, 056112 (2005)

9) Boozer, A.H. Phys. Rev. Lett. **86**, 5059 (2001)

10) A. Garofalo, et al., Phys Plasmas **10**, 4776 (2003)

11) R. Fitzpatrick, Phys. Plasmas **9**, 3459 (2002)

12) M. Shilov, et al., Phys. Plasmas **11**, 2573 (2004)

13) G.W. Hammett, F.W. Perkins, Phys. Rev. Lett. **64**, 3019 (1990)

3. Experimental run plan

Describe experiment in detail, including decision points and processes

A shot which has a similar poloidal cross-section to that produced in DIII-D during the corresponding experiment which can reach $\beta_N > \beta_N^{\text{no-wall}}$ is required for this experiment. This requires a LSN discharge with I_p = 1.0 MA, κ = 2-2.1, $\delta_{upper} \leq 0.35$, $\delta_{lower} \leq 0.6$, $l_i \sim 0.8$, with a period of $\beta_N > \beta_{N\ \text{no-wall}}$ and no large tearing modes longer than a few wall times (~150 ms minimum, >300 ms desired) to be developed. EFIT equilibrium reconstructions of the DIII-D target discharges developed during the March 17 run will be used to provide operational guidance. 4.5 kGauss TF is desirable to suppress tearing modes. Beam power and timing will be adjusted to maintain $\beta_N^{\text{no-wall}} < \beta_N < \beta_N^{\text{with-wall}}$. Modulation of the beam sources will be used to provide half-steps in the power level (no beam voltage adjustments). The no-wall and ideal-wall beta limits are expected to be ~4.8 and ~7 respectively, and will be calculated during the run using DCON once the target has been developed. If desired, a secondary I_p ramp will be used to maintain ℓ_i in the range of 0.7-0.9.

The shape of a lower single null (LSN) NSTX discharge was matched on DIII-D during the February 14 and March 17, 2005 run days (Figure 2). This is a higher kappa configuration than is typically used to conduct RWM experiments in DIII-D. Equilibria from this run provide the target shape for the NSTX run.

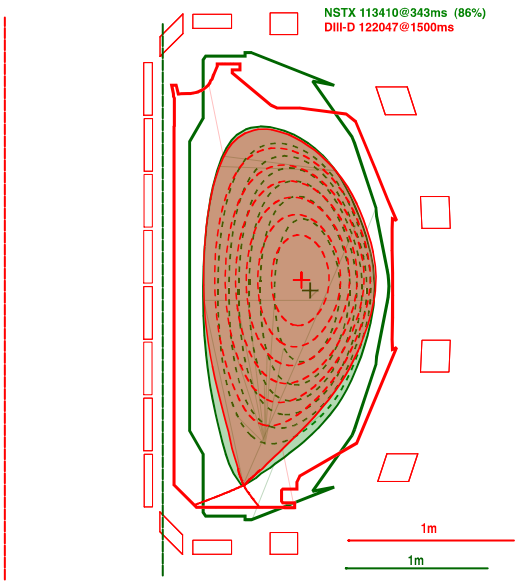

Figure 2: Comparison of scaled and translated DIII-D and NSTX poloidal cross-sections

Once a similar shot is established, guidance from XP 501 will be used to perform the experiments listed below in an efficient manner. This XP will provide a basis for operation of the error field correction coil to control RWM stability by controlling rotation damping, and perform RFA analysis with n=1 error fields. The approximate magnitude and waveform of the applied error field for sufficient rotation braking to allow an accurate determination of Ω_{crit} and the frequency range and amplitude of interest for RFA analysis will be determined from XP501.

The n = 1 braking field will be applied in steps with the flat-top for each step lasting ~50 ms unless XP501 indicates that a shorter period is adequate for field soak-in. The details of the SPA waveforms can't be determined until after XP501 is run and the target has been developed. Once XP 501 has been run, the amplitudes of the SPA currents can be determined. Once the target is developed the turn on times duration of steps and pulses of the various waveforms will be determined. Below are schematic versions of the waveforms.

n = 1 braking waveforms with 50 ms steps:

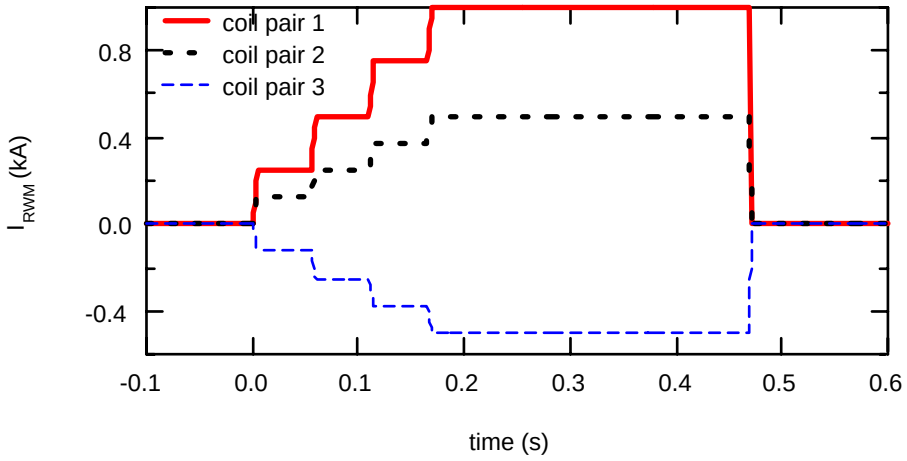

n = 1 static RFA waveforms:

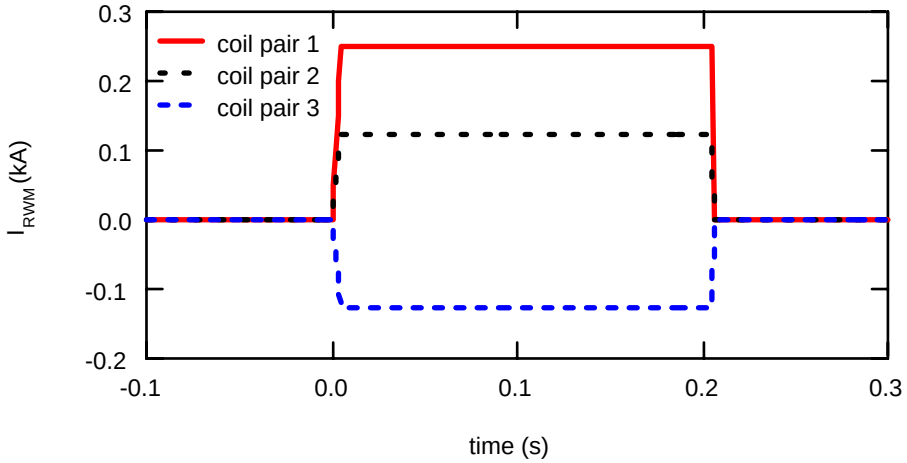

n = 1 rotating RFA waveforms (10Hz):

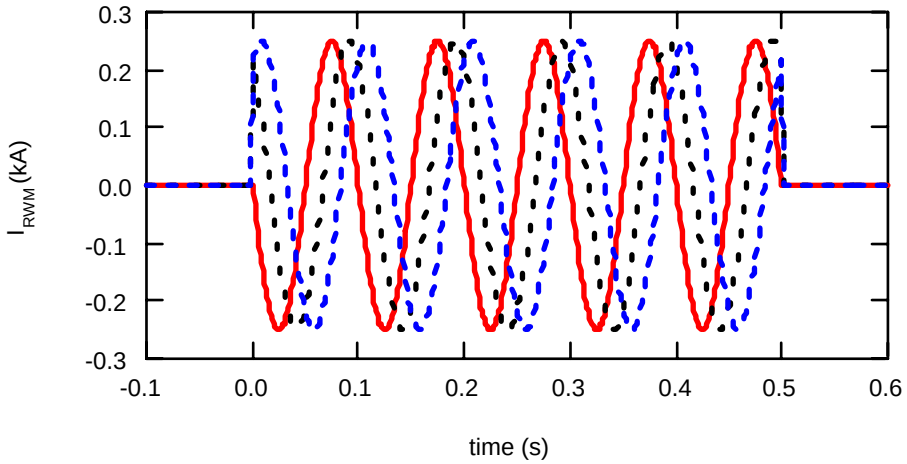

Run Plan: (48 shots total)

Task	Number of Shots
1) Establish DIII-D similar shot - Ip = 1.0 MA, LSN, κ = 2.1, δ = 0.5 with as long of period with $\beta_N > \beta_{N\ no\text{-}wall}$ as possible without large tearing modes. Use secondary I_p ramp to maintain constant ℓ_i if necessary (estimated q_{95} = 5.5)	5
2) Aspect ratio dependence of Ω_{crit}	
a. Apply DC n=1 error field to target in steps until RWM destabilized during MHD quiescent period with $\beta_N > \beta_{N\ no\text{-}wall}$ – Use XP501 for braking field guidance – $\Delta t_{step} \geq 5\tau_{wall}$ if possible - will be determined by target characteristics ($\Delta t_{step} \geq 2\tau_{wall}$ is minimum)	3
b. Adjust beam power to get β_N scaling – Adjustment will be determined based on proximity to no-wall and with-wall limits of initial target – Modulate sources rather than beam voltage adjustment if possible	6
c. Scan q_{95} by varying I_p – try to match DIII-D edge-q values: $3.6 \leq q_{95} \leq 5.4$ I_p = 0.9 MA, 0.8 MA, 0.7 MA, 0.6 MA – if I_p ramp then vary timing of braking to get variation in q_{95}	8
d. repeat (a) with fewer NBI sources for $\beta_N < \beta_{N\ no\text{-}wall}$	2
3) RWM growth rate and mode rotation frequency dependence on A & β_N -apply static & rotating error field, $\beta_N > \beta_N^{no\text{-}wall}$	
a. scan rotation frequency of applied field on initial target i. take guidance from XP 501 for frequencies ii. scan frequencies around expected peak response frequency	9
b. repeat at freq. of max. response with $\beta_N < \beta_N^{no\text{-}wall}$	2
c. apply static field to observe RFA dependence on β_N i. use DC pulse lengths short enough and field magnitudes low enough that RWM is not destabilized ii. adjust beams to vary β_N	5

– Adjustment will be determined based on proximity to no-wall and with-wall limits of initial target

4) Ω_{crit} dependence on v_A and C_s
   – adjust B_T and I_p together for const. q
   – use n=1 braking to induce RWM
   – try to maintain T_i and T_e

   a. scale down TF from best shot of day so far 8

Ip	Bt
890 kA	0.4 kGauss
775 kA	0.35 kGauss
670 kA	0.3 kGauss

Total 48

4. Required machine, NBI, RF, CHI and diagnostic capabilities

Describe any prerequisite conditions, development, XPs or XMPs needed.
Attach completed Physics Operations Request and Diagnostic Checklist

All standard magnetic diagnostics are required as well as diamagnetic loop and Thomson scattering for partial kinetic EFIT reconstructions. CHERS is required since rotation profiles are an essential part of this experiment. The internal RWM sensors will be necessary to determine onset of RWM growth. Any additional constraints to the q-profile which will be available will increase the certainty of the stability boundary mapping. This experiment will also require the RWM feedback coil to be operated in a pre-programmed mode in order to apply the external n=1 field. XP 501 should be run first to gain experience with MHD spectroscopy.

5. Planned analysis

What analysis of the data will be required: EFIT, TRANSP, etc.

Partial kinetic EFIT, including rotation effects will be performed for this experiment. DCON will be used to determine the no-wall and with-wall beta limits. MARS-F will provide detailed calculation of the magnitudes of the various dissipative and inertial terms in the RWM dispersion relation.

6. Planned publication of results

What will be the final disposition of the results; where will results be published and when?

An aspect ratio comparison of RWM stability characteristics would serve to validate the physics models used to describe the RWM and could be suitable for PRL, or for publication in Physics of Plasmas or Nuclear Fusion.

PHYSICS OPERATIONS REQUEST

NSTX - DIII-D RWM Similarity Experiment **OP-XP-512**

Machine conditions (specify ranges as appropriate)

I_{TF} (kA): **0.3-4.5kG** Flattop start/stop (s): **_____/_____**

I_P (MA): **0.6-1.0 MA** Flattop start/stop (s): **_____/_____**

Configuration: **Lower Single Null**

Outer gap (m): **0.11** Inner gap (m): **0.1**

Elongation κ: **2.1** Triangularity δ: **0.5**

Z position (m): **0.00**

Gas Species: **D / He**, Injector: **Midplane / Inner wall**

NBI - Species: **D**, Sources: **A/B/C**, Voltage (kV): **90kV** Duration (s): **_1s__**

ICRF – Power (MW): **__0__**, Phasing: **Heating / CD**, Duration (s): **_____**

CHI: **Off**

Either: List previous shot numbers for setup: **108420**

Or: Sketch the desired time profiles, including inner and outer gaps, κ, δ, heating, fuelling, etc. as appropriate. Accurately label the sketch with times and values.

DIAGNOSTIC CHECKLIST
NSTX - DIII-D RWM Similarity Experiment OP-XP-512

Diagnostic	Need	Desire	Instructions
Bolometer – tangential array			
Bolometer array - divertor			
CHERS	×		
Divertor fast camera			
Dust detector			
EBW radiometers			
Edge deposition monitor			
Edge pressure gauges			
Edge rotation spectroscopy		×	
Fast lost ion probes - IFLIP			
Fast lost ion probes - SFLIP			
Filtered 1D cameras			
Filterscopes			
FIReTIP			
Gas puff imaging			
Infrared cameras			
Interferometer - 1 mm			
Langmuir probe array			
Magnetics - Diamagnetism	×		
Magnetics - Flux loops	×		
Magnetics - Locked modes	×		
Magnetics - Pickup coils	×		
Magnetics - Rogowski coils	×		
Magnetics - RWM sensors	×		
Mirnov coils – high frequency		×	
Mirnov coils – poloidal array		×	
Mirnov coils – toroidal array		×	
MSE	×		ok to run if MSE unavailable for extended period
Neutral particle analyzer			
Neutron measurements		×	
Plasma TV	×		
Reciprocating probe			
Reflectometer – core			
Reflectometer - SOL			
RF antenna camera			
RF antenna probe			
SPRED			
Thomson scattering	×		
Ultrasoft X-ray arrays	×		
Visible bremsstrahlung det.			
Visible spectrometers (VIPS)			
X-ray crystal spectrometer - H			
X-ray crystal spectrometer - V			
X-ray PIXCS (GEM) camera			
X-ray pinhole camera			
X-ray TG spectrometer			